

Supporting Information

Tuning Partial-Charged Pt^{δ+} of Atomically Dispersed Catalysts toward Superior Propane Dehydrogenation Performance

*Wei Zhang,^{ab} Hongfei Ma,^b Haizhi Wang,^a Jiawei Jiang,^a Zhijun Sui,^{*a} Yi-An Zhu,^a De Chen,^{*b}*

Xinggui Zhou^a

^a State Key Laboratory of Chemical Engineering, East China University of Science and Technology,

130 Meilong Road, Shanghai 200237, China

^b Department of Chemical Engineering, Norwegian University of Science and Technology, Trondheim

7491, Norway

*Corresponding author:

Zhijun Sui

Tel: +86-021-6425-2169; E-mail: zhjsui@ecust.edu.cn;

De Chen

Tel: +47-735-93149; E-mail: de.chen@ntnu.no

List of contents

1. Catalyst preparation

2. Catalyst characterization

3. Catalyst evaluation

Table S1. Physical properties of Pt catalysts on various supports.

Table S2. Curve-fitting parameters for Pt 4f_{7/2} XPS spectra of fresh-reduced catalysts.

Table S3. Acidity scale for various metal oxides and important values

Table S4. The selectivities of products over various catalysts

Figure S1. Plots of time vs propane conversion over five different supports.

Figure S2. The catalytic performance of atomically dispersed Pt catalysts on various supports.

Figure S3. Schematic illustration of the relationship between the initial TOF and the peak shift of (a) Pt²⁺ and (b) Pt⁴⁺ for atomically dispersed Pt catalysts on various supports, where the solid line is the trend line.

Figure S4. the propylene selectivity obtained with three oxide-supported catalysts as a function of the acid-base character of the support material, represented by the relative Lewis acidity, $N_M - 2\delta_M$.

Figure S5. Typical HAADF-TEM images of the spent catalysts, after 4h of PDH reaction. (a) Pt/AC (b) Pt/CNTs (c) Pt/G-6, (d) Pt/TiO₂, and (e) Pt/CeO₂.

Figure S6. TG curves of the spent Pt/G-6 catalyst using different carrier gases, after 40 h of PDH reaction.

1. Catalyst preparation

The activated carbon (AC) support, purchased from Sinopharm Chemical Reagent Co. Ltd, was used directly without further treatment. The carbon nanotubes (CNTs) support was purchased from Beijing Cnano Technology Co. Ltd. About 0.5 g pristine CNTs were treated by 200 mL mixed acid solution containing 8 mol/L H₂SO₄ (Shanghai Lingfeng Chemicals, 98%) and 8 mol/L HNO₃ (Shanghai Lingfeng Chemicals, 65%) in an ultrasonic bath of 60 °C for 2 h, and then further treated by at 800 °C under Ar atmosphere (20 mL/min) for 2 h with a heating rate of 10 °C/min. The silicon-based CARiCT G-6 support was produced by Japan Fuji Silysia Chemical. The purchased G-6 was ground carefully and then dried at 120 °C for 12 h, followed by calcining in the air at 600 °C for 2 h with a heating rate of 5 °C/min. The pristine TiO₂ material was commercial rutile TiO₂ (Shanghai Titan technology Co. Ltd, 99.9%). The CeO₂ support was synthesized using the precipitation method. Ce(NO₃)₃·6H₂O (Sinopharm Chemical Reagent Co. Ltd, 99.0%) was dissolved in deionized water under stirring constantly, and then 10% NaOH (Sinopharm Chemical Reagent Co. Ltd) was added into the solution until a pH value of 10 was obtained. Afterward, the precipitates were repeatedly rinsed with a large amount of deionized water and ethanol and dried at 80 °C for 24 h. Finally, the cerium dioxide-dried precursor powders were calcined in air at 350 °C for 4 h with a heating rate of 5 °C/min.

All the supported Pt catalysts were prepared by the incipient-wetness impregnation method. Typically, an aqueous solution of H₂PtCl₆·6H₂O (Sinopharm Chemical Reagent Co. Ltd, 99.5%) was added dropwise onto 1.00 g of supports under manual stirring. After the impregnation, the samples were dried at 110 °C for 12 h, as unreduced catalyst precursors. The platinum loadings of all catalysts were used to give nominal loadings of 0.1 wt%, which were denoted as Pt/AC, Pt/CNTs, Pt/G-6, Pt/TiO₂, and Pt/CeO₂.

2. Catalyst characterization

N₂ adsorption/desorption isotherms were performed on a Micromeritics ASAP 2010 at -196 °C, with all samples degassed in vacuum for 4 h at 240 °C. Surface areas of the samples were analyzed by the multipoint Brunauer–Emmett–Teller (BET) analysis method in the $P/P_0 = 0.05–0.30$ pressure range. An inductively coupled plasma atomic-emission spectrometer (ICP-AES, Agilent Varian 710-ES) was applied to analyze the Pt contents. CO chemisorption (CO-Chem) was carried out using an Autochem-II 2920 analyzer (Micromeritics) equipped with a thermal conductivity detector (TCD). For CO-Chem, approximately 0.20 g catalyst was loaded into a U-shaped quartz tube and heated to 550 °C for 100 min under pure H₂ (20 mL/min) and then cooled to 45 °C in pure Ar (20 mL/min), and then CO pulses (10% CO/Ar) were injected to begin testing. The dispersion of platinum was estimated by CO chemisorption amount assuming the adsorption stoichiometry of CO/Pt=1. X-ray photoelectron spectroscopy (XPS) was performed on a Thermo Scientific Escalab 250Xi spectrometer equipped with an Al K α ($h\nu = 1486.71$ eV) radiation source. The binding energy was calibrated using the C 1s peak (284.6 eV) of surface adventitious carbon. The aberration-corrected high-angle annular dark-field scanning transmission electron microscopy (HAADF-STEM, JEOL JEM-ARM200F) was performed to obtain atomic resolution imaging. The thermogravimetric analysis (TGA) was performed on a PerkinElmer Pyris 1 TGA instrument to determine the amount of coke, in oxygen and nitrogen atmospheres. The sample was dried at 120 °C for 2 h, and then the temperature was increased to 800 °C at a heating rate of 10 °C/min.

In situ diffuse reflectance infrared Fourier-transform spectra of CO (CO-DRIFTS) adsorbed on catalysts was acquired with PerkinElmer Spectrum 100 FTIR spectrometer equipped with liquid nitrogen-cooled MCT detector at a spectral resolution of 4 cm⁻¹ and the scanned

wavenumber was ranged from 4000 to 400 cm^{-1} . In a typical CO-DRIFTS procedure, about 50 mg of the sample was reduced at 550 $^{\circ}\text{C}$ in pure H_2 (20 mL/min) for 100 min and then cooled to 30 $^{\circ}\text{C}$ under pure Ar (20 mL/min) for collecting a background spectrum. Afterward, 2% v/v CO/Ar (20 mL/min) was introduced for 30 min to ensure steady-state conditions. An Ar (20 mL/min) purge was performed to remove gas-phase CO from the DRIFTS cell and then spectra of chemisorbed CO were recorded continuously during the process.

3. Catalytic evaluation

The propane dehydrogenation reaction was carried out on a $\mu\text{BenchCAT}$ reactor (Altamira Instrument) under 1 bar. Typically, 0.10 g of the catalyst was loaded in the center of a quartz tube with an inner diameter of 6 mm, and reduced at 500 $^{\circ}\text{C}$ in flowing pure H_2 (20 mL/min) for 100 min with a heating rate of 10 $^{\circ}\text{C}/\text{min}$. Thereafter, mixed gases ($\text{H}_2/\text{C}_3\text{H}_8=0.8$ v/v, Argon balance, 78 mL/min) were introduced to the reactor, which gives a $\text{WHSV}_{\text{propane}}=18.9 \text{ h}^{-1}$, and the catalyst was tested at 575 $^{\circ}\text{C}$ for 4 h. The analyses of reactant and product components were analyzed online with a 4-channel Micro-GC (INFICON 3000). The conversion of propane and selectivity toward propylene were calculated as:

$$\text{Conversion} = \frac{F_{\text{C}_3\text{H}_8, \text{in}} - F_{\text{C}_3\text{H}_8, \text{out}}}{F_{\text{C}_3\text{H}_8, \text{in}}} \times 100\%$$

$$\text{Selectivity} = \frac{F_{\text{C}_3\text{H}_6, \text{out}}}{\sum_i \frac{n_i}{3} F_{i, \text{out}}} \times 100\%$$

Where $F_{\text{C}_3\text{H}_8, \text{in}}$ is the flow rate of propane in the feed; $F_{\text{C}_3\text{H}_8, \text{out}}$, $F_{\text{C}_3\text{H}_6, \text{out}}$, and $F_{i, \text{out}}$ are the flow rates of propane, propylene, and component i in the outlet; and n_i is the carbon number of component i .

The diffusion-free operation was examined experimentally by varying space velocities and catalyst particle sizes. Results showed that, under these reaction conditions, the external and internal diffusion effects were safely excluded under the reaction conditions adopted here. The TOF was calculated as:

$$TOF = \frac{(F_{in} - F_{out}) M}{mLD}$$

Where F_{in} is the molar flow rate of propane in the feed (mol/s) ; F_{out} is the molar flow rate of propane in the outlet (mol/s); M is the molar mass of Pt (g/mol); m is the amount of the catalyst (g); L is the loading amount of Pt (%); D is the dispersion of Pt (%). The initial values of the reactions were used (under a low propane conversion < 15%).

Table S1. Physical properties of Pt catalysts on various supports.

Sample	Pt loading (wt%) ^a	S _{BET} (m ² /g) ^b	V _{pore} (cm ³ /g) ^b	D _{pore} (nm) ^b	Pt dispersion ^c
Pt/AC	0.1	1397	0.95	3.2	>99%
Pt/CNTs	0.1	224	1.35	25.2	>99%
Pt/G-6	0.1	499	0.72	5.3	>99%
Pt/TiO ₂	0.1	16.8	0.03	42.9	>99%
Pt/CeO ₂	0.1	74.6	0.23	14.0	>99%
Pt/Al ₂ O ₃ ^d	0.1	67.8	0.35	20.3	~97%

^a Determined by ICP-AES. ^b Calculated from N₂ adsorption/desorption experiments. ^c Determined by CO chemisorption at 45 °C with assuming CO/Pt = 1. ^d Cited from reference [1].

Table S2. Curve-fitting parameters for Pt 4f_{7/2} XPS spectra of fresh-reduced catalysts.

Sample	Pt ⁴⁺			Pt ²⁺			The normalized oxidation state of Pt ^b
	B.E (eV)	Area (%)	Peak shift ^a	B.E (eV)	Area (%)	Peak shift ^a	
Pt/AC	73.9	25	-0.7	72.4	75	0	2.50
Pt/CNTs	74.0	30	-0.6	72.6	70	0.1	2.60
Pt/G-6	74.3	45	-0.3	72.9	55	0.4	2.90
Pt/TiO ₂	74.5	49	-0.1	73.2	51	0.7	2.98
Pt/CeO ₂	74.8	68	0.2	73.5	32	1.0	3.36

^a The shift of Pt^{δ+} peak, and the standard Pt 4f_{7/2} binding energy of Pt²⁺ and Pt⁴⁺ are 72.4 eV and 74.6 eV, respectively. ³⁶

^b The average oxidation state of Pt = 4*Y_{Pt4+} + 2*Y_{Pt2+}, where the Y is the area fraction.

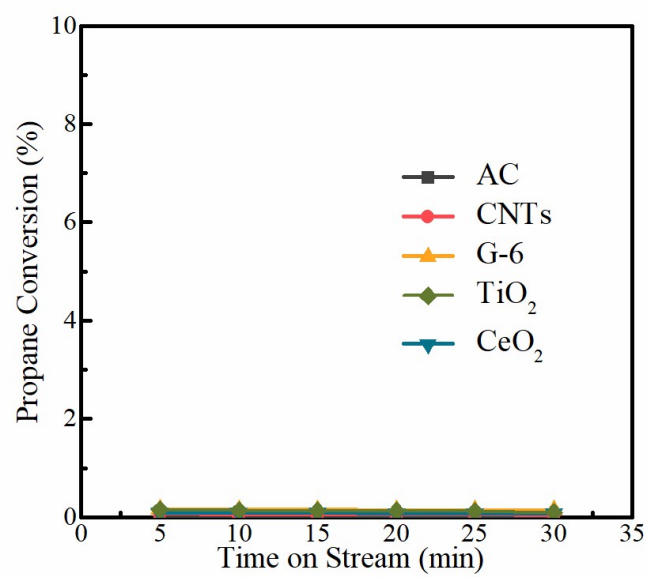


Figure S1. Plots of time vs propane conversion over five different supports.

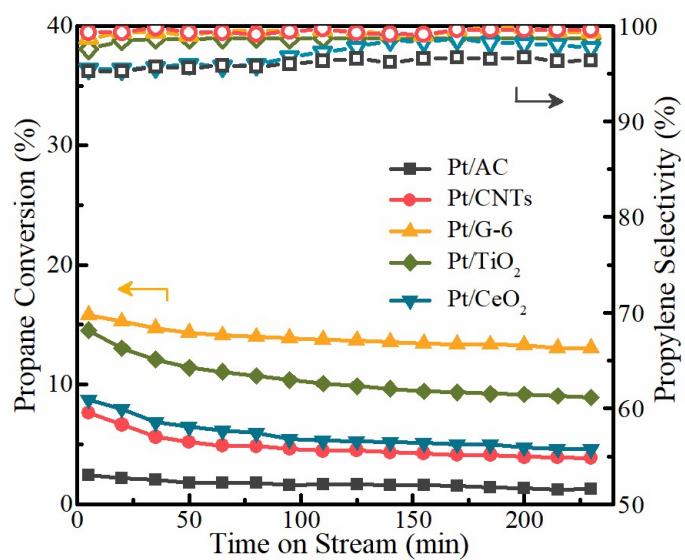


Figure S2. The catalytic performance of atomically dispersed Pt catalysts on various supports. Reaction conditions: 0.1 g of the catalyst, $P = 1$ atm, $T = 575$ °C, $H_2/C_3H_8 = 0.8$ v/v, argon balance, $V_{total} = 78$ mL/min, and $WHSV_{propane} = 18.9$ h⁻¹.

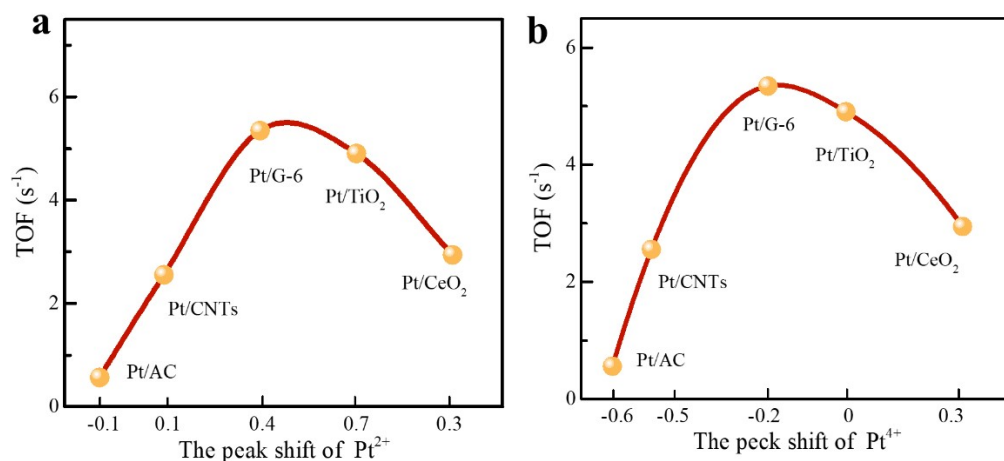


Figure S3. Schematic illustration of the relationship between the initial TOF and the peak shift of (a) Pt^{2+} and (b) Pt^{4+} for atomically dispersed Pt catalysts on various supports, where the solid line is the trend line.

Table S3. Acidity scale for various metal oxides and important values

M_xO_y	S_M	S_{Ch}	δ_M	N_M	$N_M-2\delta_M$
SiO ₂	2.140	3.645	0.511	4	2.978
TiO ₂	1.500	3.645	0.477	4	3.046
CeO ₂	0.410	3.645	0.203	4	3.594

Sandersons partial charges of the metal ions (δ_M) are expressed by Equation (S1) for the metal oxides (M_xO_y):

$$\delta_M = \frac{\sqrt{(x+y)(S_{M^{n+}})^x (S_{Ch})^y} - S_{M^{n+}}}{2.08\sqrt{S_{M^{n+}}}} \quad (S1)$$

where $S_{M^{n+}}$ and S_{Ch} represent Sandersons Electronegativity of the metal in the oxidation state of n^+ and Sandersons Electronegativity of the chalcogen, respectively.

N_M represents the formal oxidation state of the metal in a compound. The values of $N_M-2\delta_M$ can be readily derived from their stoichiometries and the Sandersons EN values of the component elements can serve as a scale for surface acidities of various metal oxides. The more positive the number, the stronger (Lewis) acidic strength.^{2, 3}

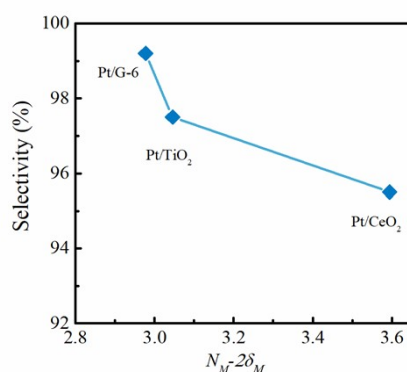


Figure S4. the propylene selectivity obtained with three oxide-supported catalysts as a function of the acid-base character of the support material, represented by the relative Lewis acidity, $N_M-2\delta_M$.

Table S4. The selectivities of products over various catalysts

Sample	Selectivity (%) ^a			
	CH ₄	C ₂ H ₄	C ₂ H ₆	C ₃ H ₆
Pt/AC	0	1.97	2.28	95.5
Pt/CNTs	0	0.7	0.3	99.0
Pt/G-6	0	0.3	0.5	99.2
Pt/TiO ₂	0	1.00	1.5	97.5
Pt/CeO ₂	3.3	0.9	0.3	95.5

^a The initial value.

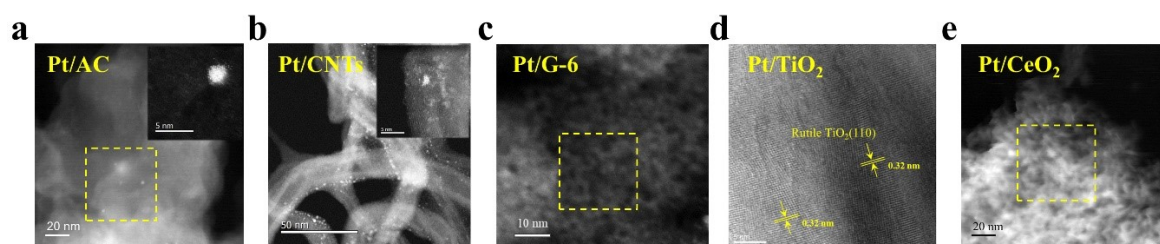


Figure S5. Typical HAADF-TEM images of the spent catalysts, after 4h of PDH reaction. (a) Pt/AC (b) Pt/CNTs (c) Pt/G-6, (d) Pt/TiO₂, and (e) Pt/CeO₂.

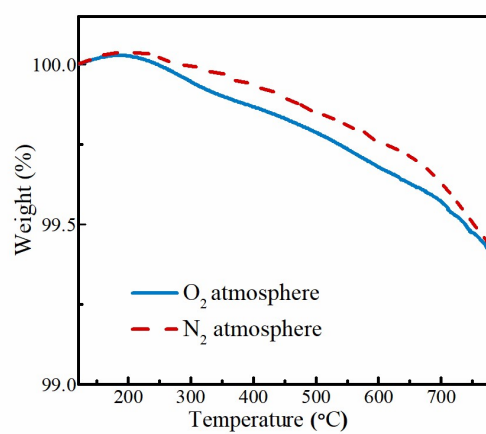


Figure S6. TG curves of the spent Pt/G-6 catalyst using different carrier gases, after 40h of PDH reaction.

Reference

- (1) Zhang, W.; Wang, H.; Jiang, J.; Sui, Z.; Zhu, Y.; Chen, D.; Zhou, X. Size dependence of Pt catalysts for propane dehydrogenation: from atomically dispersed to nanoparticles. *ACS Catal.* **2020**, *10*, 12932-12942.
- (2) Jeong, N. C.; Lee, J. S.; Tae, E. L.; Lee, Y. J.; Yoon, K. B., Acidity scale for metal oxides and Sanderson's electronegativities of lanthanide elements. *Angew. Chem. Int. Ed.* **2008**, *47* (52), 10128-10132.
- (3) Sanderson, R., Electronegativity and bonding of transitional elements. *Inorg. Chem.* **1986**, *25* (19), 3518-3522.